International Journal of Bifurcation and Chaos, Vol. 15, No. 9 (2005) 2995–3009

MODELING BONE RESORPTION IN 2D CT AND 3D μCT IMAGES

A. ZAIKIN* and J. KURTHS
Institute of Physics, University of Potsdam, D-14415 Potsdam, Germany
**Department of Mathematical Sciences, University of Exeter, EX4 4QE Exeter, UK*

P. SAPARIN and W. GOWIN
Center of Muscle and Bone Research, Department of Radiology and Nuclear Medicine, Charité-University Medicine Berlin, Hindenburgdamm 30, D-12203 Berlin, Germany

S. PROHASKA
Zuse Institute Berlin (ZIB), Takustr. 7, 14195 Berlin, Germany

Received May 27, 2004; Revised September 28, 2004

We study several algorithms to simulate bone mass loss in two-dimensional and three-dimensional computed tomography bone images. The aim is to extrapolate and predict the bone loss, to provide test objects for newly developed structural measures, and to understand the physical mechanisms behind the bone alteration. Our bone model approach differs from those already reported in the literature by two features. First, we work with original bone images, obtained by computed tomography (CT); second, we use structural measures of complexity to evaluate bone resorption and to compare it with the data provided by CT. This gives us the possibility to test algorithms of bone resorption by comparing their results with experimentally found dependencies of structural measures of complexity, as well as to show efficiency of the complexity measures in the analysis of bone models. For two-dimensional images we suggest two algorithms, *a threshold algorithm* and *a virtual slicing algorithm*. The threshold algorithm simulates bone resorption on a boundary between bone and marrow, representing an activity of osteoclasts. The virtual slicing algorithm uses a distribution of the bone material between several virtually created slices to achieve statistically correct results, when the bone-marrow transition is not clearly defined. These algorithms have been tested for original CT 10 mm thick vertebral slices and for simulated 10 mm thick slices constructed from ten 1 mm thick slices. For three-dimensional data, we suggest a variation of the threshold algorithm and apply it to bone images. The results of modeling have been compared with CT images using structural measures of complexity in two- and three-dimensions. This comparison has confirmed credibility of a virtual slicing modeling algorithm for two-dimensional data and a threshold algorithm for three-dimensional data.

Keywords: Modeling bone resorption; complexity; virtual slicing algorithm.

1. Introduction

Due to the rapid development of computer techniques, numerical modeling of pathological processes in medicine at the cellular level will soon become an important tool in the early phases of clinical studies. This will allow us to simulate *in silico* the effect of cell's activation much faster than in laboratory tests or clinical measurements. Simulations of the bone architecture and its evolution can be essential for the following problems: (i) prediction of the bone loss due to osteoporosis or microgravity conditions for space-flying personnel; (ii) providing test objects for newly developed structural measures; (iii) understanding physical mechanisms behind the bone alteration. For an adequate mathematical description of the bone dynamics, several different approaches have been used so far, e.g. modeling resorption with Basic Multicellular Units (BMUs) [Langton *et al.*, 1998, 2000], which represent osteoclast and osteoblast cell populations, application of artificial structures to simulate the bone [Langton *et al.*, 1998], modeling by replication of voxels schemes [Sisias *et al.*, 2002], modeling with idealized trabecular structure [Jensen *et al.*, 1990], or stochastic simulation of bone dynamics, based on histomorphometry data [Thomsen *et al.*, 1994]. Several algorithms and procedures have been reported to evaluate the influence of mechanical loading on the architecture of trabecular bone. These works have shown that changes of a bone structure depend on the distribution of the mechanical load [Huiskes *et al.*, 2000; Ruimerman *et al.*, 2003] and have suggested methods to evaluate and simulate the mechanical strength of the given bone architecture [Gunaratne *et al.*, 2002]. Finally, an attempt has been carried out to describe the formation of the bone tissue on a microscopic level using reaction–diffusion equations [Tabor *et al.*, 2002]. Despite numerous studies of bone models, there is no commonly-accepted algorithm that adequately describes bone dynamics.

We suggest a new approach and develop several algorithms to simulate bone mass loss *directly* from two-dimensional (2D) computed tomography (CT) and three-dimensional (3D) micro-computed tomography (μCT) bone images. Noteworthy are the two crucial distinctions of our modeling approach from previously reported ones. First, the modeling algorithms developed here can work with original CT bone images in 2D or 3D, i.e. we start with the analysis of original CT or μ-CT images, model the bone resorption and produce simulated bone images. Second, we use recently developed structural measures of complexity (SMC) [Gowin *et al.*, 1998] as an evaluation tool to quantify different aspects of the bone architecture and its evolution along the simulation of the bone mass loss. This approach demonstrates also the efficiency of these SMC [Saparin *et al.*, 1998; Gowin *et al.*, 1998, 2001; Saparin *et al.*, 2005] to evaluate changes in a bone architecture.

The paper is structured as follows. First, we describe three sets of experimental data, i.e. bone images, used for numerical simulations of bone dynamics and for comparison with simulation results. Next, we introduce three algorithms to model bone resorption: *threshold algorithm* (TA), *virtual slicing algorithm for 2D* (VSA), and *threshold algorithm for 3D* (TA 3D). After that, we briefly review structural complexity measures used for the quantification of the modeling results. Then we discuss the application of these algorithms for different sets of data, compare simulations with CT acquisitions, and summarize the results.

2. Materials

For modeling bone resorption in bone images we have used the following bone images:

- *Data set 1*: 2D bone images of human vertebra. The central axial slices of 1 mm thickness were acquired from nonfractured human lumbar vertebrae L3 specimens using a CT-scanner Somatom Plus S (Siemens AG). Vertebral bodies were examined by high-resolution computed tomography (HRCT) applying an image matrix of 512×512 pixels and an in-plane pixel resolution of 0.182×0.182 mm. For each vertebra, 10 continuous central slices had been taken. The specimens were from females (mean age 71 years) and from males (mean age 67 years). For every vertebra ten 1 mm thick slices had been merged into one 10 mm thick slice, mimicking the application of clinical quantitative computed tomography (QCT) with the same in-plane resolution. After this procedure, there is the possibility to model the bone resorption both for 10 mm slices as well as for every 1 mm slices with subsequent averaging into a 10 mm slice (Fig. 1).
- *Data set 2*: 2D bone images of human vertebra. The L3 vertebrae from human specimens were scanned on a CT scanner (Somatom Plus 4, Siemens AG). One 10 mm thick transaxial center

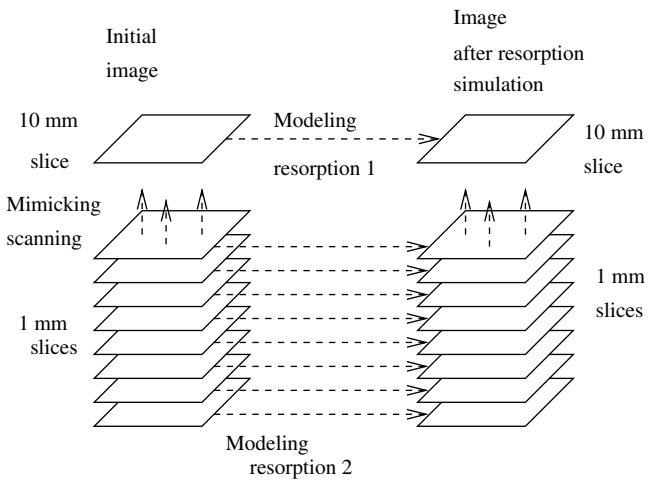

Fig. 1. Different opportunities to model bone resorption in 2D. If the initial image (left) is represented by a set of high resolution 1 mm thick slices, we can merge them and average to obtain a low resolution 10 mm thick slice (left up). After that, we can model resorption both in this low resolution 10 mm thick slice or in each of the high resolution 1 mm thick slices, then merge 1 mm thick slices and compare the results.

slice of each specimen was obtained. It had 0.192×0.192 mm in-plane image resolution and was represented by a 512×512 matrix. These 10 mm thick slices were obtained by QCT resulting in the assessment of the BMD. The bone mineral density (BMD) of the specimens ranged from 3.8 to 103.5 mg/cm^3. Here and for the *data set 1* the original CT-image was processed with a segmentation algorithm to segment the surrounding soft issue from the vertebral bone (for details see [Saparin *et al.*, 1998]). After that, an application of a separation algorithm segmented the vertebral body into the cortical bone and the trabecular bone. Only the trabecular bone was used for modeling.

- *Data Set 3*: 3D bone images of human tibia biopsies. 24 biopsies were taken from the proximal tibia specimens harvested from the same human cadavers at the medial side 17 mm distal of the tibia plateau. This location is a surgical site for harvesting trabecular bone grafts. The biopsies were obtained with a surgical diamond coring drill with the utmost care and the best possible precision. Biopsies had a shape of a cylinder with a diameter of 7 mm, the length of the biopsies varied between 20 and 40 mm. The biopsies were scanned with a micro-CT scanner μCT 40 at Scanco Medical AG, Switzerland, using a voxel size of $20 \times 20 \times 20\,\mu$m. The resulting gray-scale images were segmented using a low-pass filter to remove noise, and a fixed threshold filter to extract the mineralized bone phase.

3. Modeling Algorithms

To model bone resorption, several algorithms have been developed, based on the procedure, proposed by Langton *et al.* [Langton *et al.*, 1998] for 2D artificial lattices of bone images. This algorithm simulates the activity of the basic multicellular units (BMUs), which consist of a population of osteoclasts and osteoblasts. The algorithm describes a random activation of BMU, its movement and resorption of bone material, and termination of its activity after a random time. A BMU is activated on the surface of the trabecular structure. Hence, to simulate its activation, one should exactly determine the border between bone material and marrow. This is a difficult task for thick 2D CT images because computed tomography produces partial volume effects resulting in pixel values averaged over a 3D volume determined by the slice thickness. We suggest a solution to overcome this difficulty by means of a virtual slicing algorithm.

3.1. *Threshold algorithm in 2D*

One of the most straightforward algorithms that can be used for simulation of the bone mass loss and consequent architectural changes in 2D bone images is a *threshold algorithm* (TA). We introduce TA as a sequence of the following steps. First, a threshold T is chosen experimentally to separate a bone image, represented by the matrix $A(i, j)$ of X-ray well-defined attenuations, into bone and marrow pixels. After this, the border between marrow and bone is well defined, and we simulate the activation of BMUs on this border. The pixel (i, j) belongs to the border when its attenuation $A(i, j)$ is larger than T (a bone pixel) and one of its four neighbors belongs to the marrow, $A(i, j) < T$. One iteration step includes the following procedures: (i) For every pixel belonging to the bone-marrow border, we generate a random number uniformly distributed in the range $[0, 1]$. (ii) If this random number is larger than the activation frequency of BMU F_a, then the BMU will be activated in the area, which includes this pixel and its four neighbors. (iii) During the activation the BMU resorbs some constant amount of the bone material, called the resorption unit RU, and then its activity is terminated.

After one iteration step in the area of the BMU activity, the new attenuation of the pixel (i, j) will be equal to $A(i, j) - RU$. After several iteration steps N_s the bone image is saved for visualization and further analysis. The modeling terminates when all pixels have an attenuation smaller than T, or the requested mean attenuation is achieved. This algorithm produces a set of bone images with decreasing bone mineral density (BMD) and can be used for the comparison with experimentally obtained bone images having different BMDs. The TA algorithm can be applied to both 10 mm and 1 mm slices. In the latter case one can expect better results due to a more precisely defined border between bone and marrow.

3.2. *Virtual slicing algorithm in 2D*

The reason why sometimes TA does not model bone resorption similarly to the observed data, is the absence of a sharp transition between bone and marrow in the 2D CT image. This can lead to a very artificial inhomogeneous bone mass loss. To avoid this problem, we have developed a *virtual slicing algorithm* (VSA), which models resorption for bone images without sharp transition between bone and marrow.

The key idea of this algorithm is the following (see Fig. 2): To find a clear border between bone and marrow, we reconstruct a 3D bone image by means of virtual slices. We represent the initial bone image by N virtual slices and for every pixel of the bone image (e.g. Fig. 2, left) we randomly distribute the intensity A of this pixel in N virtual slices (e.g. Fig. 2, middle). In L slices the pixel value is set to bone, in the remaining $N - L$ slices this pixel is set to an attenuation value representing marrow. The parameters $N = 10$ and $L = 5$ are fixed. Since the distribution of the material between virtual slices occurs in a random way, every stochastic realization corresponds to a different material distribution. Three examples of this distribution for one pixel, obtained for three different realizations, are presented in Fig. 2 (right).

Now, the TA algorithm can be conveniently applied in every virtual slice due to a ten times smaller slice thickness resulting in the clearly defined bone-marrow border. After modeling resorption in each virtual slice, the results are again averaged over all virtual slices into an image with lower resolution. This final image with decreased average attenuation represents the simulated bone loss provided by the VSA algorithm. Noteworthy, due to their stochastic origin, virtual slices cannot be compared with original high resolution CT-slices, i.e. this algorithm does not perform a real reconstruction of the 3D structure (as in [Pollefeys *et al.*, 1999]) from one thick 2D slice. The distribution of the bone material between virtual slices is only statistically correct but rules of architectural connectivity are not respected.

In detail, the algorithm is applied by means of the following subsequent procedures. The attenuation of the initial pixel $A(i, j)$ is randomly distributed among N virtual slices. For every pixel the average over all virtual slices is equal to the pixel value in the initial bone image, while at the same time each virtual slice has the defined border between bone and marrow. For every pixel $A(i, j)$ of the initial bone image, we put the intensity of the bone material $B(i, j, k)$ in slice k, $k = 1 \ldots L$, randomly chosen from L bone-receiving slices. Each

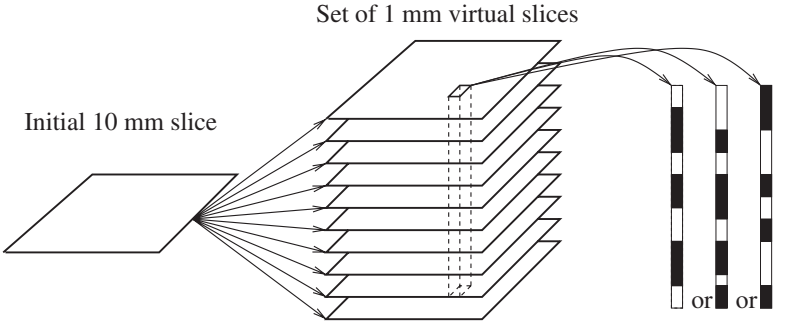

Fig. 2. The virtual slicing algorithm to model bone mass loss with dynamic stochastic simulation. (Left) A starting point is the bone image without sharp transition between bone and marrow. (Middle) The bone material is distributed over several virtual slices. (Right) Three examples of the random bone material distribution for one pixel, resulting from three different stochastic realizations.

slice from N slices has the same probability to be chosen in L bone-receiving slices. In the remaining $(N-L)$ slices we set the value of appropriate pixel to the intensity of the marrow threshold M. The distribution is performed with respect to the principles of computed tomography, to fulfill the condition

$$A(i,j) = \frac{1}{N}\left(\sum_{k=1}^{L} B(i,j,k) + (N-L)M\right). \quad (1)$$

To achieve this condition, we calculate a minimum A_{MIN} of the pixel attenuations $A(i,j)$ inside the trabecular bone. If A_{MIN} is significantly smaller as predefined marrow threshold T_g (e.g. in bones images with fat) and the aim is strictly to avoid resorption below T_g, the parameter A_{MIN} may be set equal to T_g. For every pixel $A(i,j)$ of the initial bone image in k slice of L randomly chosen bone-receiving slices we place the value $B(i,j,k) = A_{\mathrm{MIN}} + (A(i,j) - A_{\mathrm{MIN}} + \xi_k)N/L$, where ξ_k are mutually uncorrelated Gaussian distributed random numbers with variance σ^2. The remaining $(N-L)$ intensities are set the value $M = A_{\mathrm{MIN}}$. Finally, the small difference between $NA(i,j)$ and $(\sum_{k=1}^{L} B(i,j,k) + (N-L)A_{\mathrm{MIN}})$ is added to the first slice $B(i,j,1)$ to fulfill condition (1) for every pixel. As a result, we get virtual slices with a defined border between bone and marrow in each slice. We model the resorption in each slice separately, applying TA with the threshold $T = A_{\mathrm{MIN}}$ to decrease the values $B(i,j,k)$, and average slices after N_s iteration steps according to the expression (1). The resorption in each pixel of each slice is performed until its attenuation $B(i,j,k)$ will be smaller as predefined given threshold T_g.

3.3. *Threshold algorithm in 3D*

To model osteoporotic changes in the 3D bone images in a realistic way, we have developed a simple algorithm that describes a deterioration of the trabecular structure. For the algorithm we have taken the idea of the algorithm proposed by Langton [Langton *et al.*, 1998]. To extend this algorithm into 3D, we have used the following approach. We set a threshold T separating bone and marrow. Then, modeling of the resorption is performed in several steps. Each step includes the following procedures: we mark all surface voxels on the border between bone and marrow, and then remove these surface voxels with some probability P_r, that corresponds to the random activation of BMU. By surface voxels, we understand voxels which are located on the border between bone and marrow belonging to the bone. These voxels have the attenuation larger than T but at least one of six neighboring voxels belongs to marrow (attenuation below T). By application of this algorithm we have avoided the necessity to model the activity of BMUs on a 3D surface.

4. Nonlinearity and Complexity of the Trabecular Structure

Often viewed by layman as a static support system, the human skeleton is in fact a dynamic organ, that is as much as other organic systems involved in the information processing that characterizes human physiology. Information known about trabecular bone structure, obtained by different structure analysis methods or computational finite element modeling, suggests its architecture is highly nonlinear and complex. Trabecular bone appears to be arranged as a geometrical nonlinear structure [Stölken & Kinney, 2003]. The interdependency of function and form in biological systems [Thompson, 1992] can be found in particular in the skeleton. The concept of structural stability and its adaptive evolution as described by Kauffman [1993] is a modern delineation of the historical work by D. W. Thompson. The complexity and nonlinear architecture of the trabecular bone maintains its stability through adaptive processes coming from outside of the skeletal system. The biomechanical load applied to the bones and their ability to react upon it suggests a system that is self-organizational. This process has been studied [Kauffman, 2000]. Although it seems to be obvious for the skeleton, the notion and the mechanisms of self-organization of the bone are not yet fully understood. Recent experimental results have given strong indications that geometric nonlinearities within the complex architectural arrangement can play an important role in failure of trabecular bone [Townsend *et al.*, 1975; Kopperdahl & Keaveny, 1998]. It remains an open question at what volume fraction or spatial arrangement the geometric nonlinearity becomes biomechanically important and are these transitions affected by ageing, disease or drug treatment [Keaveny, 2004].

Following the suggestion that the structure of trabecular bone can be regarded as a complex system [Complex systems, 2001; Lakes, 1993; Olson, 1997], we apply measures of complexity to analyze quantitatively the 2D and 3D structural

composition of the trabecular bone structure. The apparent structure of the trabecular bone can be considered in a model that is based on 2D and 3D CT-images as Cellular Nonlinear Network in which the pixels or voxels representing the trabecular bone may be interpreted as 2D or 3D arrays of mainly locally connected nonlinear dynamical subunits, whose dynamics are functionally determined by a small set of parameters [Chua & Yang, 1988; Chua & Roska, 1993]. In the present study we describe the evolution of the trabecular structure with nonlinear stochastic algorithms.

The resulting parameters are complexity measures which characterize a system with many interacting and interrelating components and assess the trabecular bone structure responsible for the bone functionality and skeletal dynamics. Interactions between subunits of the complex trabecular bone system lead to the emergence of new collective nonlinear properties of the bone system as a whole. The collective behavior of certain parts of the system implies that this activity is a property of the whole system, but not a property of its single parts [Weinberg, 1992; Stewart, 1998]. The complexity of the bone architecture manifested, for example, in the collective property of the trabecular subunits to bear the mechanical load, can be adequately characterized by structural measures of complexity, as proposed in [Saparin *et al.*, 1998; Gowin *et al.*, 1998, 2001] and also applied here.

5. Quantification of the Bone Structure in 2D and 3D

We apply structural measures of complexity (SMC) to quantify the bone architecture. The development of the complexity analysis in 2D is described in [Saparin *et al.*, 1998; Gowin *et al.*, 1998, 2001] in detail. Hence, here we only give a brief review of this technique. The segmented CT-image, representing only the trabecular bone, is transformed by means of symbolic dynamics into a symbol-encoded image. The purpose of symbol encoding is to reduce the amount of information in the bone image, but leave important aspects of the bone architecture intact. In 2D five symbols have been used for symbol encoding (three static L, V, H and two dynamical symbols I, C). Image encoding substitutes the original pixel values by one of these five different symbols; the encoding is based on both the dynamics and the level of X-ray attenuation in the vicinity of an encoded pixel [Saparin *et al.*, 1998].

After symbol encoding, five structural measures of complexity are used to quantify different aspects of the bone architecture [Saparin *et al.*, 1998]. These measures utilize probability distributions of local quantities and entropy-based calculations from the symbol-encoded images:

1. The architectural composition is expressed in the Index of Global Ensemble (IGE), which is a ratio between positive and negative structural elements. This measure is calculated as $\mathrm{IGE} = [p(I) + p(C)]/[p(L) + \varepsilon]$, where $p(I)$, $p(C)$ and $p(L)$ denote probability of the corresponding symbols, and ε is a predefined small constant to avoid division by zero.
2. The organization of the connected marrow space surrounding the trabecular network is expressed by the size of the maximal L-block.
3. To calculate the other three measures we use a small window, which moves through the image. For every window we calculate the probabilities of different symbols. Then the Structure Complexity Index (SCI) measures the interregional complexity of the trabecular composition, and is calculated as the Shannon entropy for the distribution of index of the local ensemble ILE, where
$$\mathrm{ILE} = \frac{p(I) + p(C)}{p(L) + \varepsilon},$$
and the result is also normalized by the maximal value of Shannon entropy $S_{\max}$ achievable for a partition used to construct the distribution. The higher SCI, the more nonuniform and complex is the structure.
4. The disorder of the trabecular composition is assessed by the Structure Disorder Index (SDI), which is calculated as the Shannon entropy of the 3D distribution in the space $\{p(L),\ p(I + C),\ p(V + H)\}$. All probabilities used here are normalized by the corresponding probability normalization condition. The less ordered is the structure, the larger is the SDI.
5. The organization of hard elements (with higher values of attenuation or edges) within the structure, i.e. the homogeneity of the trabecular connection, is quantified by the Trabecular Net Index (TNI). To calculate TNI, the median M_e and the Shannon entropy S_h of the distribution of local trabecular quantities $p(V) + p(I) + p(C)$, calculated from every position of moving

window, are determined. Then

$$\mathrm{TNI} = \frac{M_e}{\frac{S_h}{S_{\max}}},$$

where $S_{\max}$ is the maximal value of the entropy for a given number of distribution bins used to construct the distribution.

In 3D, another method of symbol encoding is used, because here there is a sharp transition between bone and marrow. Following this fact, in 3D the symbol encoding is based on an alphabet of three different symbols [Saparin *et al.*, 2005], which represent marrow M, bone surface (one voxel thick) S, and internal bone I. Three measures have been applied to quantify the bone image: Structure Complexity Index (SCI 3D), and a normalized probability density of the trabecular surface $P(S)$, and internal bone $P(I)$ voxels inside the bone image. SCI 3D is introduced similarly to 2D [Saparin *et al.*, 1998] and quantifies the complexity of symbol compositions between different regions of the bone, whereas $P(S)$ and $P(I)$ define the probabilities of the bone surface voxels and the internal bone voxels normalized by the total number of bone voxels.

6. Modeling Bone Resorption in 2D

We start with the data set 1, that contains ten axial 1 mm thick slices from the central part of each vertebra. 50 vertebral bones with a BMD from 21 [mg/cm^3] to 122 [mg/cm^3] were analyzed. Mimicking the QCT vertebral image, we merge these slices into one 10 mm thick slice. This enables us to model bone deterioration in two ways: (i) either model resorption directly on 10 mm slice (modeling resorption 1 in Fig. 1), or (ii) simulate loss of bone mass in each 1 mm slice, and then merge the result again into a final 10 mm slice (modeling resorption 2 in Fig. 1). We start with an application of TA for 10 mm thick vertebral images with the parameters: $T = 76$ HU, $F_a = 0.97$, $RU = 1$ and $N_s = 1100$. The parameter N_s denotes the number of simulation steps between saved iterations. Using this algorithm, we have produced 25 bone images with decreasing mean attenuation. Iterations 0, 5, 11 and 25 are visualized in Fig. 3 and demonstrate that TA produces very inhomogeneous resorption of the bone material within the trabecular structure.

To verify and quantify the results of the resorption simulations, we have calculated structural complexity measures for the simulated vertebral images. These dependencies versus the decreasing mean attenuation are shown in Fig. 4, where they are compared with osteoporotic vertebral images with corresponding mean attenuation. This comparison shows that even such a simple algorithm is able to model nonlinear behavior of SMC and qualitatively reproduce the results obtained from osteoporotic vertebrae. However, quantitatively the simulation results differ from the osteoporotic dependencies, and even a variation of simulation parameters in a wide range cannot provide a good matching. The reason for this is the highly inhomogeneous resorption of the trabecular bone. Setting the threshold selects some regions in the attenuation landscape, but the resorption of the bone evolves like a propagation of a wave front, and this is unrealistic.

The main reason why TA does not work adequately, is the difficulty to determine the exact border between bone and marrow in 10 mm 2D CT bone images. In 1 mm thick slices this border is *a priori* better defined due to smaller partial volume effects for thin slices. Hence, we have checked modeling of the resorption in each 1 mm thick slice with consequent merging of the results into 10 mm thick slices. Note that the vertebral image, used as a starting point for modeling, differs from the corresponding 10 mm thick slice (compare iteration 0 in Figs. 3 and 5). This fact results from the segmentation procedure applied to each 1 mm thick slice. If we separate a trabecular structure in each of the 1 mm thick slices, and then merge the results into a 10 mm thick slice, the result will differ from those of first merging all slices of 1 mm thickness and then segmenting the trabecular bone from the cortical shell. The reason is the slightly different location of the cortical shell in each slice due to concave spatial shape of a vertebra. Applying TA in each of the 1 mm thick slices and merging the results, we get 25 simulated bone images with decreasing mean attenuation. The parameters of TA applied to each slice were $T = 76$ HU, $F_a = 0.97$, $RU = 10$ and $N_s = 110$. The iterations $0, 5, 11$ and 25 are presented in Fig. 5. In this case resorption occurs not so abruptly but nevertheless very inhomogeneously. The comparison between the structure of original CT osteoporotic and simulated vertebral slices is given in Fig. 6 and demonstrates better agreement between simulated and CT images. A disagreement occurs because this resorption simulation leads to the

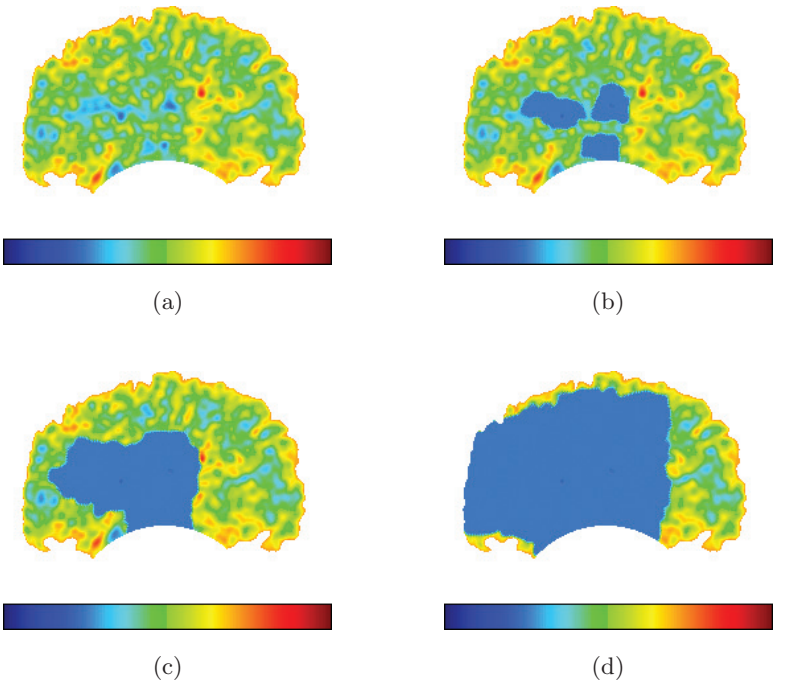

Fig. 3. Application of the threshold algorithm to simulate bone resorption in 2D for the merged 10 mm thick vertebral slices from data set 1: iteration steps $0, 5, 11$ and 25 (a–d). Images are coded with a color scale $(-24, 376)$ HU. This algorithm produces very inhomogeneous resorption of the bone material.

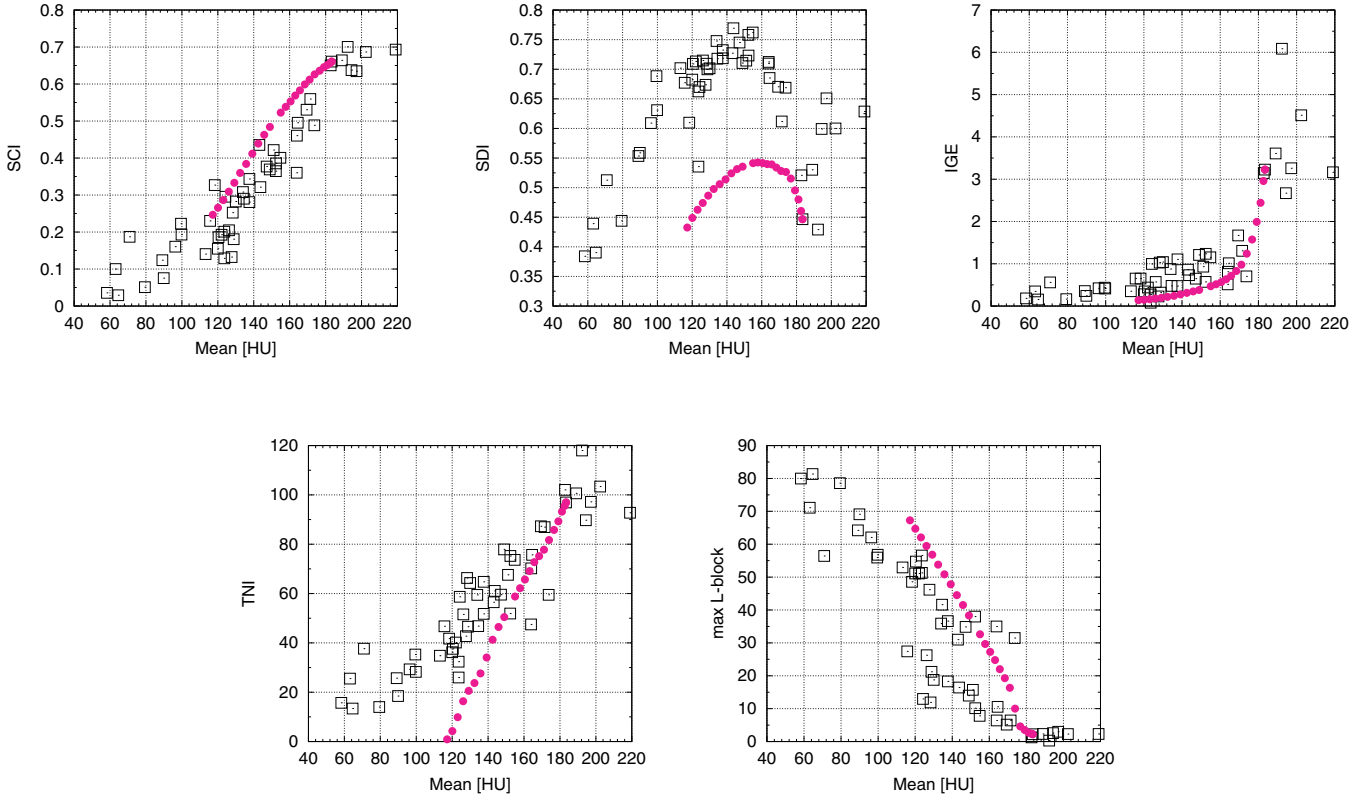

Fig. 4. Comparison between simulated bone loss in 10 mm thick merged slices (circles), made with TA, and osteoporotic changes in vertebrae assessed from original 10 mm thick CT-images (squares). Different measures of complexity, plotted against the mean attenuation (HU), quantify distinct aspects of bone architecture: structural complexity index (SCI), structural disordering index (SDI), index of global ensemble (IGE), trabecular net index (TNI), and maximal L block (max L-block).

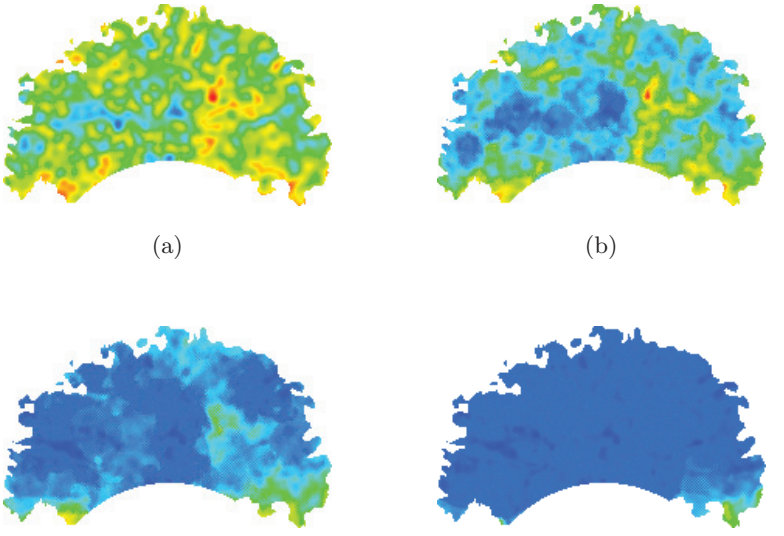

(a) (b)

(c) (d)

Fig. 5. Modeling of bone resorption, applying TA algorithm in each original CT 1 mm thick slice with consequent merging of these slices into a 10 mm thick slice. The resulting 10 mm thick slices are shown from left to right for iteration steps 0, 5, 11 and 25 (a–d). Images are coded as in Fig. 3.

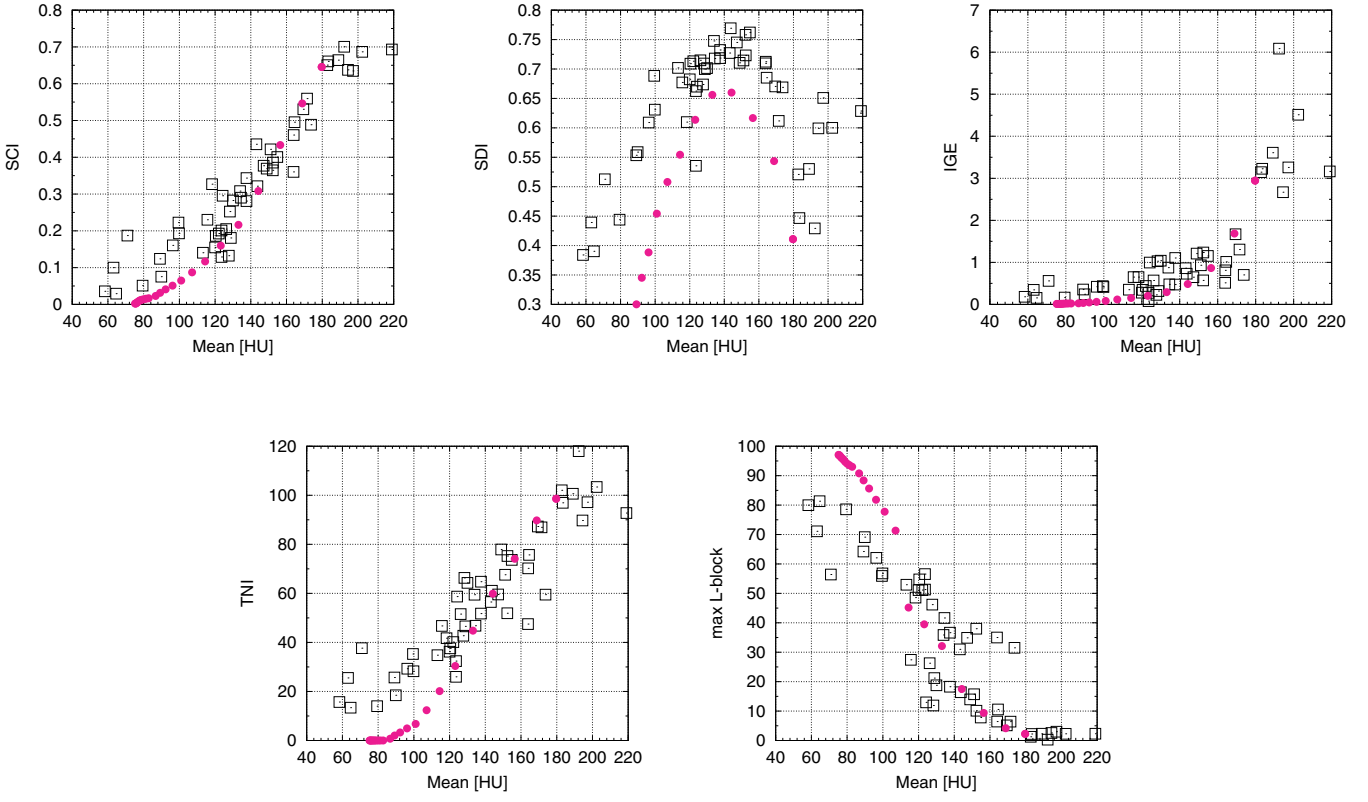

Fig. 6. Application of SMC for a comparison between original CT images of vertebrae with different variations of osteoporosis (squares) and images averaged over ten 1 mm thick slices, simulated with TA (circles).

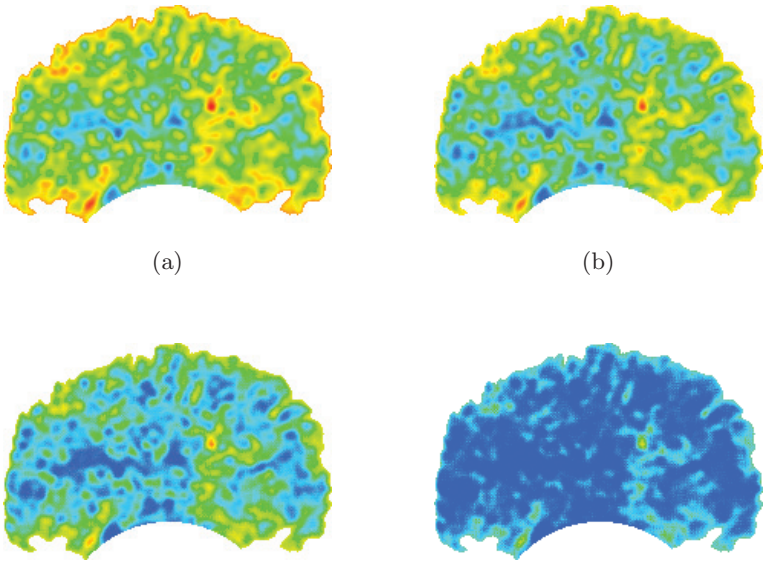

Fig. 7. Modeling of bone deterioration with the virtual slicing algorithm in merged 10 mm thick slices. Original (a) and simulated (b–d) bone images of one vertebra are shown from left to right for iteration steps 0, 5, 11 and 25. Images are coded as in Fig. 3.

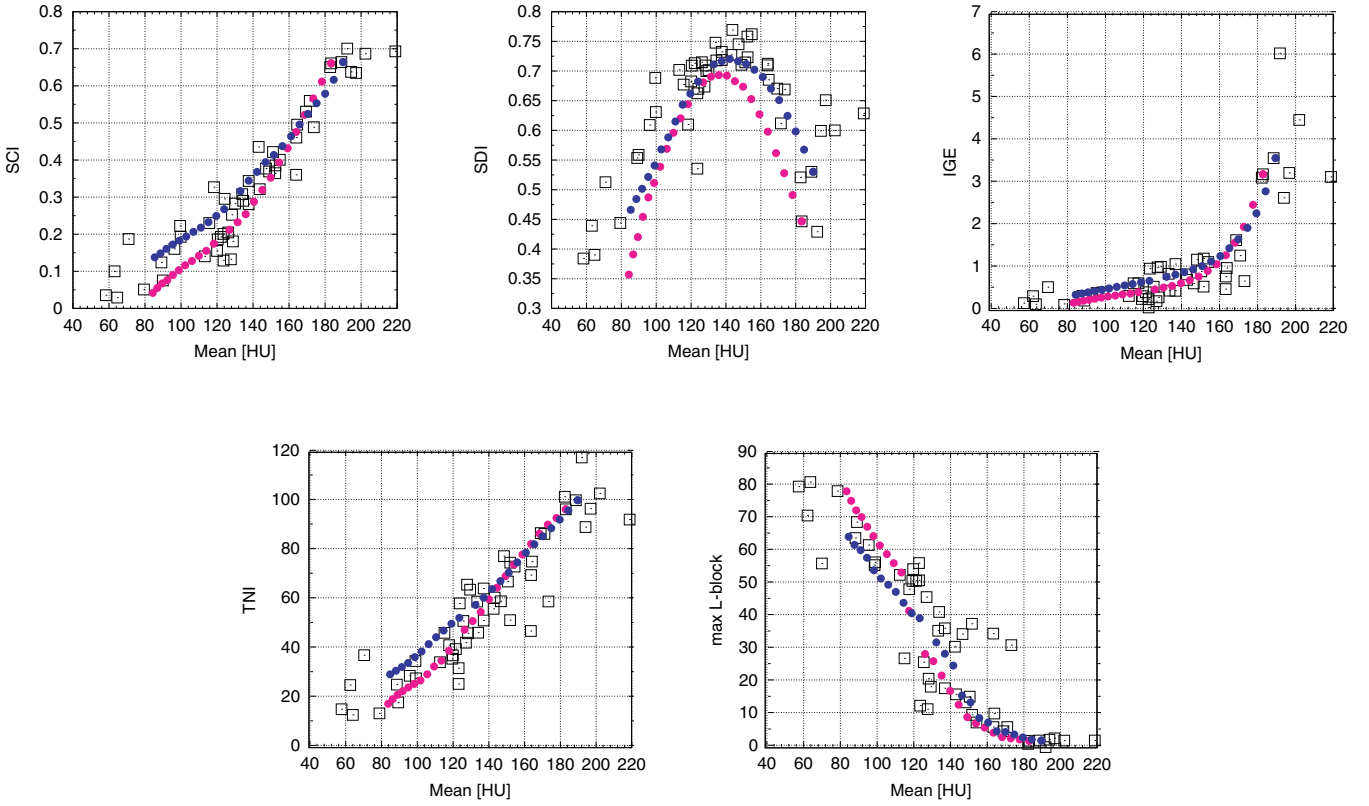

Fig. 8. The relation between the mean attenuation (HU) and the complexity measures during the loss of bone mass in osteoporotic vertebra (original CT images, squares) and in the images simulating bone resorption using VSA (circles, magenta and blue colors represent two different initial vertebral images).

appearance of a large area with small attenuation, due to the application of TA algorithm in each slice.

Modeling bone resorption in each of the 1 mm thick slices is not always possible in practice, because usually clinical measurements are performed with larger slice thickness. Therefore, we have developed the virtual slicing algorithm (VSA), which constructs virtual slices. We apply this algorithm to the same bone as above with parameters $T_g = -24$ HU, $\sigma^2 = 10$, $L = 5$, $N = 10$, $F_a = 0.97$, $RU = 1$ and $N_s = 75$. The vertebral structures simulated with VSA (iterations $0, 5, 11$ and 25) are presented in Fig. 7 and show that the bone resorption occurs visually in a much more realistic way. For VSA simulated changes in bone structure all simulated SMC dependencies also match very well with the dependencies for CT images (Fig. 8). To confirm this we have displayed also the results for another vertebra used as an initial point for our simulations, achieving good correspondence between osteoporotic and modeled alternations of trabecular bone.

To confirm results obtained with data set 1, we have applied TA and VSA to data set 2. This data set is represented only by 10 mm thick slices, that are closer to routine clinical bone examination. The experimentally measured dependencies of SMC qualitatively differ from dependencies of data set 1 and, hence, a verification of the algorithm has been especially interesting to check whether these algorithms are able to reproduce different experimentally observed dependencies.

We have taken a bone image with a high attenuation and applied TA with parameters $T =$ 66 HU, $F_a = 0.97$, $RU = 25$ and $N_s = 5$. Simulated bone images with mean attenuation values 158, 124.7 and 93.6 HU are shown in Fig. 9. The image [Fig. 9(a)] illustrates the application of a threshold (attenuation larger than a threshold is encoded in black). As above, we have used a trabecular region of the human vertebra, segmented from the vertebral image by the preprocessing algorithm described in [Saparin *et al.*, 1998]. It can be seen that bone deterioration occurs here very nonuniformly mainly towards the center of the image. This is not very realistic (Fig. 9). We have analyzed the comparison of the corresponding structure dependencies and found that simulations and assessment of CT images for vertebrae with different BMD do not match (Fig. 10).

The application of VSA works better and produces vertebral images with structural complexity values similar to the original CT data. The results of the simulations are visualized in Fig. 11 for mean

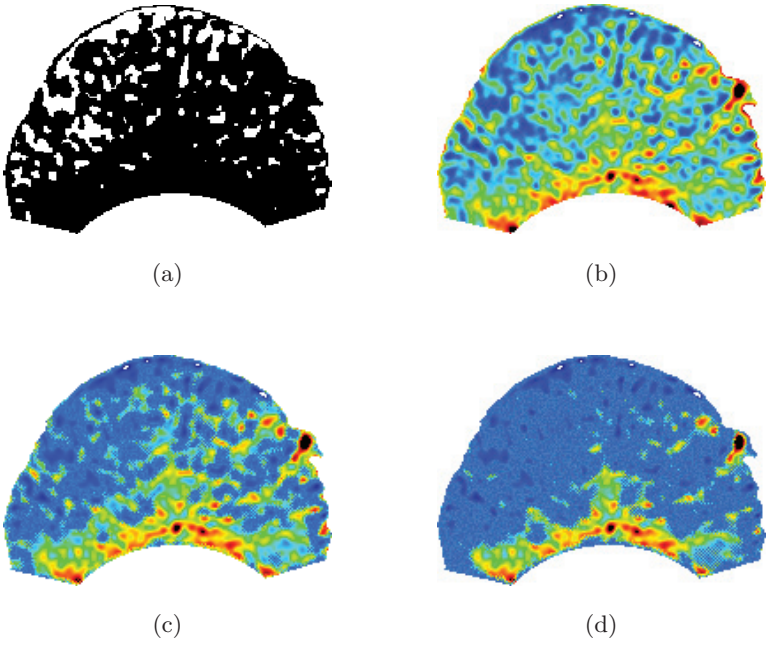

(a) (b) (c) (d)

Fig. 9. Artificial deterioration of a human vertebra from data set 2 with threshold algorithm. (a) Application of the threshold 66 HU determines a boundary between bone (black) and marrow (white). (b–d) Simulated bone images with mean attenuation values 158, 124.7 and 93.6 HU are shown. Images are coded with a "temperature" color scale from the minimum intensity −224 HU (blue) to the maximum intensity 776 HU (brown).

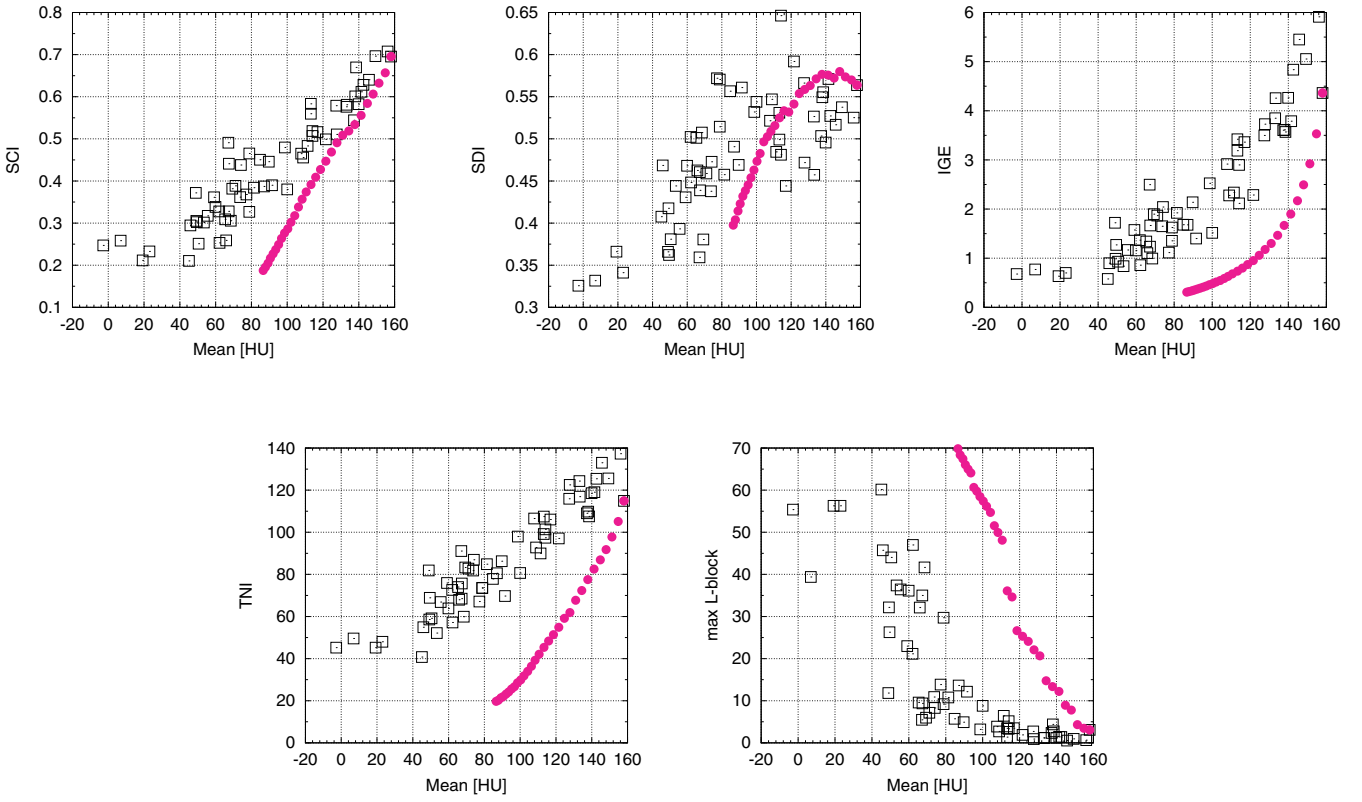

Fig. 10. SMC, assessing different aspects of the bone architecture do not demonstrate agreement between simulation using TA (circles) and original CT data (squares) results. The dependencies of SMC are plotted against the mean attenuation (HU) of the vertebrae.

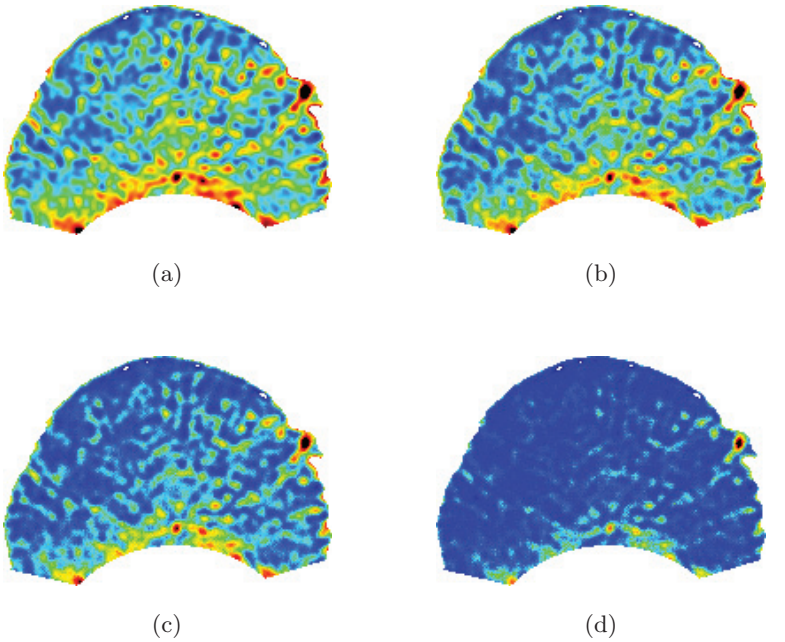

Fig. 11. Artificial deterioration of a human vertebra (data set 2) by a virtual slicing algorithm. (a–d) Simulation of the bone mass loss with mean attenuation values 158, 126.8, 83.9 and 15.2 HU. Images are encoded as in Fig. 9.

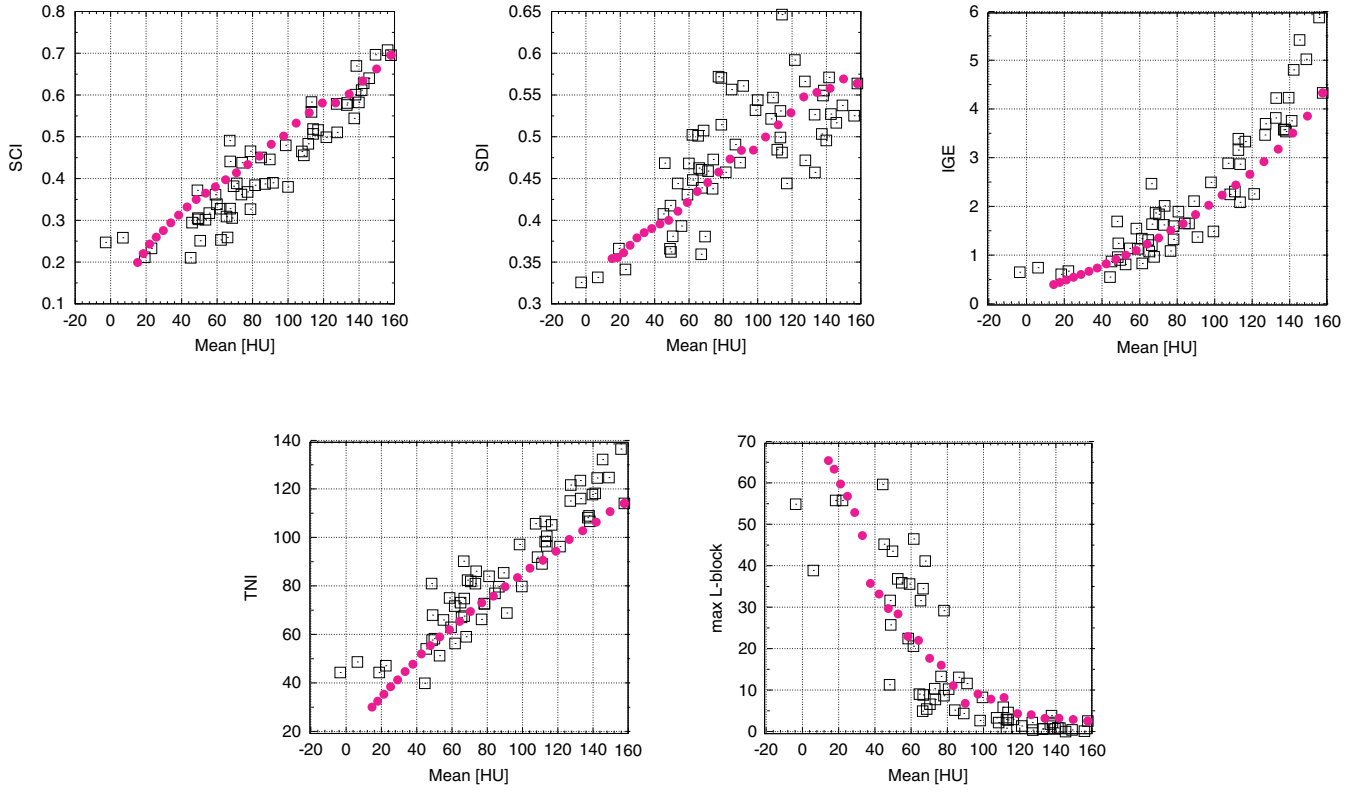

Fig. 12. SMC, evaluating different aspects of the bone architecture using VSA show good matching between simulated images (circles) and original CT images of data set 2 (squares). The dependencies of SMC are plotted versus the mean attenuation [HU] of the trabecular bone linearly related to the BMD.

attenuation values 158, 126.8, 83.9 and 15.2 HU. The application of this algorithm with parameters $T_g = 96$ in CT numbers, $\sigma^2 = 10$, $L = 5$, $N = 10$, $F_a = 0.97$, $RU = 25$ and $N_s = 5$ enables us to model the resorption in a more uniform way. The conclusion that this resorption algorithm corresponds better to the reality can be also confirmed by a comparison of structural complexity of simulated vertebrae with the original vertebral CT slices of the same mean attenuation. This comparison is presented in Fig. 12. A good matching between CT images and simulation is achieved for all five SMC. For all presented results we have tried several stochastic realizations and obtained practically identical dependencies.

7. Modeling Bone Resorption in 3D

To model changes in the trabecular bone structure in a realistic way in 3D, we have used TA 3D with the parameter $P_r = 0.001$. A visualization of the deterioration of spatial bone structure modeled with this algorithm is shown in Fig. 13(a) with a resolution of $20 \times 20 \times 20\,\mu$m. The data were visualized using the advanced 3D visualization system Amira, developed by ZIB [Zuse Institute Berlin].

Figure 13(b) shows simulated and original dependencies of SMC versus Bone-Volume-to-Total-Volume ratio (BV/TV), which is a 3D analogue of the 2D mean attenuation resulting from the analysis of biopsies. The decrease of BV/TV reflects the loss of bone mass due to a osteoporotic deterioration of the trabecular structure. A rather good correspondence was found between simulated and μCT data structures for SCI3D. With respect to the behavior of normalized probabilities $P(I)$ and $P(S)$, the model is unable to capture the fluctuations presented in the experimental dependencies. However, it can predict the point where these dependencies cross each other. This point may be responsible for the critical BV/TV value of irreversible changes, the point of no return for the bone tissue to regain structural competence. The model predicts linear dependence for these probabilities.

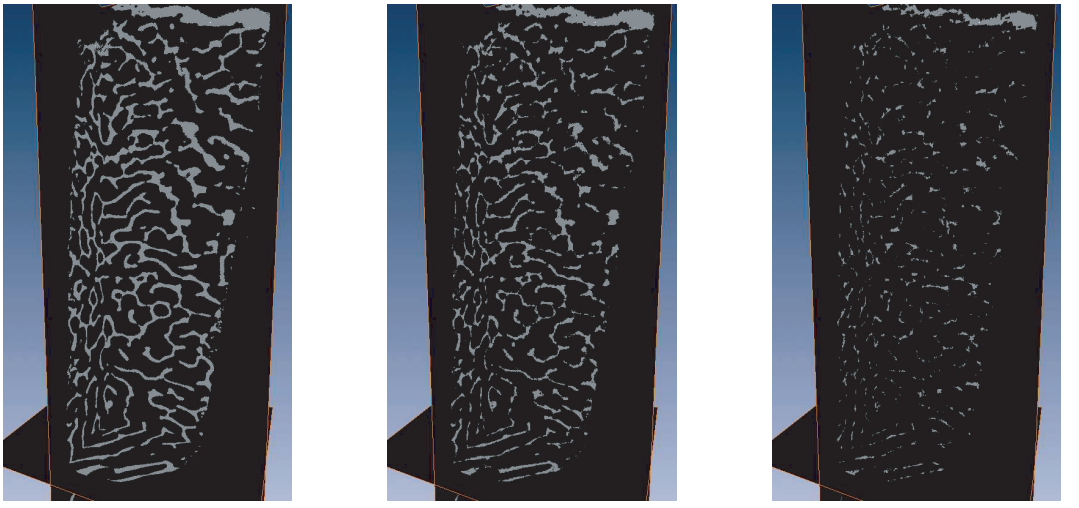

(a)

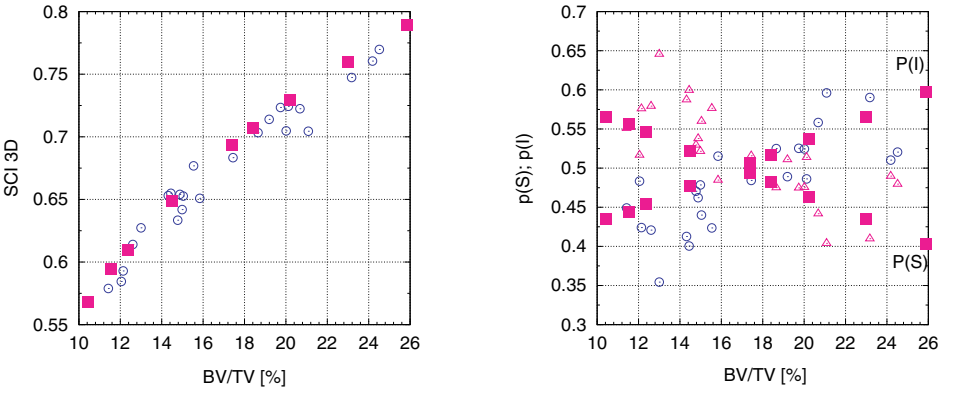

(b)

Fig. 13. (a) Artificial deterioration of a human tibia bone biopsy from data set 3 with dynamic stochastic simulation. Visualization is performed using the Amira program. The attenuation is color encoded from black (soft tissue) to white (bone). The cortical bone is on the top of image. From right to left: simulation of the bone mass loss is shown for iterations 0, 87 and 237. (b) Corresponding dependencies of SMC on BV/TV for simulation (squares) and μCT images (circles and triangles).

8. Summary

We have suggested and applied several algorithms to model loss of bone mass in 2D and 3D. For 2D vertebral CT images the best results have been obtained by the *virtual slicing algorithm*. This algorithm can be applied *directly* to bone CT-images, and it works also when there is no sharp bone-marrow transition. For 3D bone biopsy data, the threshold algorithm provides an adequate simulation of bone resorption. The comparison with original CT- and micro-CT- data in 2D and 3D performed in terms of SMC has shown a good correspondence between simulated and osteoporotic changes in bone structure and proved the credibility of the resorption algorithms for the prediction of bone loss due to osteoporosis or under the conditions of microgravity. The application of the algorithm enables us to extrapolate the dependencies of SMC to low values of BMD where experimental results might not be available. The proposed bone modeling can contribute to the development of diagnostic measures for the quantification of structural loss and, in the future, to the prediction of compositional changes of the bone tissue. We expect the simulation algorithms and comparison with acquired CT images, suggested in this paper, will be used for further investigations, including modeling a reverse process of bone formation. This approach, hence, will help to understand physical mechanisms behind the bone structural changes.

Acknowledgments

This study was made possible in part by grants from the Microgravity Application Program/Biotechnology from the Manned Spaceflight Program of the European Space Agency (ESA). The authors would also like to acknowledge Scanco Medical, Roche Pharmaceuticals and Siemens AG for support of the study.

References

Chua, L. O. & Yang, L. [1988] "Cellular neural networks: Theory and application," *IEEE Trans. Circuits Syst.* **35**, 1257–1290.

Chua, L. O. & Roska, T. [1993] "The CNN paradigm," *IEEE Trans. Circuits Syst.–I* **40**, 147–156.

Gowin, W., Saparin, P. I., Kurths, J. & Felsenberg, D. [1998] "Measures of complexity for cancellous bone," *Tech. Health Care* **6**, 373–390.

Gowin, W., Saparin, P. I., Kurths, J. & Felsenberg, D. [2001] "Bone architecture assessment with measures of complexity," *Acta Astronautica* **49**, 171–178.

Gunaratne, G. H., Rajapaksa, C. S., Bassler, K. E., Mohanty, K. K. & Wimalawansa, S. J. [2002] "A model for bone strength and osteoporotic fracture," *Phys. Rev. Lett.* **88**, 068101.

Huiskes, R., Ruimerman, R., Harry van Lenthe, G. & Janssen, J. D. [2000] "Effects of mechanical forces on maintenance and adaptation of form in trabecular bone," *Nature* **405**, p. 704.

Jensen, K. S., Mosekilde, Li. & Mosekilde, Le. [1990] "A model of vertebral trabecular bone architecture and its mechanical properties," *Bone* **11**, 417–423.

Kauffman, S. A. [1993] *The Origins of Order* (Oxford University, NY).

Kauffman, S. A. [2000] *Investigations* (Oxford University, NY).

Keaveny, T. M. [2004] "On Stölken and Kinney (Bone 2003;33(4):494–504)," *Bone* **34**, 912.

Kopperdahl, D. L. & Keaveny, T. M. [1998] "Yield strain behavior of trabecular bone," *J. Biomech.* **31**, 601–608.

Lakes, R. [1993] "Materials with structural hierarchy," *Nature* **361**, 511–515.

Langton, C. M., Haire, T. J., Ganney, P. S., Dobson, C. A. & Fagan, M. J. [1998] "Dynamic stochastic simulation of cancellous bone resorption," *Bone* **22**, 375–380.

Langton, C. M., Haire, T. J., Ganney, P. S., Dobson, C. A., Fagan, M. J., Sisias, G. & Phillips, R. [2000] "Stochastically simulated assessment of anabolic treatment following varying degrees of cancellous bone resorption," *Bone* **27**, 111–118.

Olson, G. B. [1997] "Computational design of hierarchically structured materials," *Science* **277**, 1237–1242.

Pollefeys, M., Koch, R. & Van Gool, L. [1999] "Self-calibration and metric reconstruction inspite of varying and unknown internal camera parameters," *Int. J. Comput. Vis.* **32**, 7–25.

Ruimerman, R., Van Rietbergen, B., Hilbers, P. & Huiskes, R. [2003] "A 3-dimensional computer model to simulate trabecular bone metabolism," *Biorheology* **40**, 315–320.

Saparin, P. I., Gowin, W., Kurths, J. & Felsenberg, D. [1998] "Quantification of cancellous bone structure using symbolic dynamics and measures of complexity," *Phys. Rev.* **E58**, p. 6449.

Saparin, P. I., Thomsen, J. S., Prohaska, S., Zaikin, A., Kurths, J., Hege, H. C. & Gowin, W. [2005] "Quantification of spatial structure of human proximal tibial bone biopsies using 3d measures of complexity," *Acta Astronautica* **56**, 820–830.

Stewart, I. [1998] *Life's Other Secret* (Wiley & Sons, NY).

Stölken, J. S. & Kinney, J. H. [2003] "On the importance of geometric nonlinearity in finite-element simulations of trabecular bone failure," *Bone* **33**, 494–504.

Sisias, G., Philips, R., Dobson, C. A., Fagan, M. F. & Langton, C. M. [2002] "Algorithms for accurate rapid prototyping replication of cancellous bone voxel maps," *Rapid Prototyp. J.* **8**, 6–24.

Tabor, Z., Rokita, E. & Cichocki, T. [2002] "Origin of the pattern of trabecular bone: An experiment and a model," *Phys. Rev.* **E66**, 051906.

Thomsen, J. S., Mosekilde, Li., Boyce, R. W. & Mosekilde, E. [1994] "Stochastic simulation of vertebral trabecular bone remodeling," *Bone* **15**, 655–666.

Thompson, D. W. [1992] *On Growth and Form*, the Complete Revised edition (Dover, NY).

Townsend, P. R., Rose, R. M. & Radin, E. L. [1975] "Buckling studies of single human trabeculae," *J. Biomech.* **8**, 199–201.

Weinberg, S. [1992] *Dreams of a Final Theory* (Pantheon Books, NY).

Ziemelis, K. & Allen, L. (eds.) [2001] "Complex systems," *Nature* **410**, 241–284.

Zuse Institute Berlin (ZIB) and Indeed — Visual Concepts, Berlin, *Amira 3.1 — User's Guide and Reference Manual — Programmer's Guide*, October 2003, http://amira.zib.de.